Signature of nonuniform area quantization on black hole echoes

Kabir Chakravarti,[*] Rajes Ghosh,[†] and Sudipta Sarkar[‡]
Indian Institute of Technology, Gandhinagar, Gujarat 382355, India

(Received 19 December 2021; accepted 7 February 2022; published 22 February 2022)

A classical black hole is characterized by a horizon that absorbs the radiation of all frequencies incident on it. The perturbation of these black holes is well understood via exponentially damped sinusoids known as quasinormal modes. Any departure from such classical behavior near the horizon may induce significant modifications in the late-time evolution of the perturbation leading to so-called gravitational wave echoes. This work considers the effect of black hole area quantization on the formation of gravitational wave echoes. We investigate how the resulting echo waveform may depend on various model parameters. Our study opens up a new window to distinguish different models of area quantization using future gravitational wave observations and provides a novel probe to study the near-horizon physics.

DOI: 10.1103/PhysRevD.105.044046

I. INTRODUCTION

Gravitational wave (GW) astronomy is offering us an intriguing opportunity to test the classical and quantum aspects of black holes [1,2]. In a recent work [3], the authors have suggested that the GWs emitted from black hole inspirals may carry detectable imprints of the underlying quantum mechanical properties of the horizon. This is based upon Bekenstein's proposal [4,5] of black hole area quantization: $A = \alpha l_p^2 N$, where l_p is the Planck length, N is a positive integer, and α is a constant. Such a discretization process, which could be a consequence of the Planck-scale physics, may leave its signature on the emission [5] as well as the absorption spectrum of black holes [3,6–9].

All these works crucially assume the validity of Bekenstein's entropy formula—i.e., the black hole entropy is proportional to the area of the event horizon. In general relativity (GR), this area law is motivated mainly from the Hawking area theorem [10], which states that the area of a classical black hole cannot decrease. However, once we venture beyond GR, the entropy of a black hole is no longer proportional to the horizon area, and it can have subleading correction terms [11,12]. Also, if we interpret the black hole entropy as the entanglement entropy due to the entanglement of the modes of a quantum field, the area law can be obtained by tracing over the modes hidden by the black hole horizon [13]. Interestingly, if the quantum field is in a state different from the vacuum, the entropy receives subleading corrections [14–16]. In fact, it is also proposed that, in general, only the entropy is quantized with an equally spaced spectrum [17]. If the entropy is not proportional to area, the horizon area is then quantized in a nonuniform manner.

The upshot of such a nonuniform area quantization on the phasing of gravitational waveforms from coalescing black hole inspirals is analyzed in Ref. [18]. It has been shown that any correction to the area law may lead to detectable consequences in future GW observations. Moreover, such observations may as well put severe constraints on various parameters of the underlying model. This technique also provides a novel test for the area-entropy proportionality of black hole solutions in Einstein's theory of gravity.

A natural question to ask is whether such area discretization may affect the postmerger ringdown phase. The ringdown spectrum for a classical black hole consists of the quasinormal modes which are derived using the perfectly ingoing boundary condition at the horizon. However, due to its quantized area, a black hole can only absorb at certain characteristic frequencies. This would lead to a modification of the boundary condition at the horizon. Any such modification will affect the late-time behavior of the postmerger spectrum and gives rise to so-called GW echoes.

GW echoes following the merger of compact objects have been investigated extensively in the last few years [19–24], and the possible presence of echoes in GW data is also being analyzed [25–31]. Nevertheless, the modification of the horizon boundary condition which led to the generation of these echo signals was implemented in a rather *ad hoc* fashion. However, in Ref. [7], it has been proposed that the quantization of black hole area may provide a concrete theoretical justification for the modified boundary condition at the horizon. It is modeled by adding a double-barrier potential near the horizon that mimics the selective absorption of quantum black holes. In that case,

[*]kabir.c@iitgn.ac.in
[†]rajes.ghosh@iitgn.ac.in
[‡]sudiptas@iitgn.ac.in

any future observation of GW echo in the late-time signal from a binary black hole merger could confirm the hypothesis of area quantization.

In this paper, we further develop the model proposed in Ref. [7] by introducing new perspectives. We demonstrate how the details of the area quantization can be captured by a careful choice of the double-barrier parameters that are placed to mimic the boundary condition on the horizon. It allows us to incorporate finer details of the area quantization in the echo spectrum, which was not manifest in the previous model [7]. As a consequence, our model breaks the universality of the echo time—i.e., the time difference between two consecutive echoes—and make it dependent on the model of area quantization.

Thus, our work complements the results of Ref. [7] by computing the possible effects of nonuniform area quantization on the gravitational wave echo spectrum similarly to the inspiral case studied in Ref. [18]. We use a scenario where the black hole entropy has subleading corrections in the form of a power law [14–16]. Then, by assuming the entropy is quantized in equidistant steps, we can find the nonuniform quantization rules for the horizon area:

$$A = \alpha l_p^2 N(1 + CN^{\nu}). \tag{1}$$

Here, C is a constant present in the power-law correction term in the entropy. The other parameter ν is assumed to be negative in order to get back Bekenstein's area quantization law as $N \to \infty$. It is important to emphasize that in our model, the nonuniform area quantization need not be due to additional higher-curvature terms; we continue using this model for GR black holes as well. Then, we analyze the effect of area discretization on the black hole echo spectrum.

Our work opens up a potential possibility to impose severe constraints on the choice of theoretically plausible models of area quantization using the future observation of black hole echo signals from different sources. Our study also provides another test for the area-entropy proportionality in parallel to the test presented in Ref. [18].

II. QUANTUM FILTER FOR NONUNIFORM AREA QUANTIZATION

A classical black hole absorbs any radiation incident on it. In other words, the event horizon of a classical black hole has zero reflectivity ($R = 0$) and unit transmissivity ($T = 1$). However, the situation changes drastically when the black hole's area is assumed to be quantized, as prescribed in Eq. (1). Then, it can only absorb at certain frequencies, characterized solely by the mass of a Schwarzschild black hole [3,18]:

$$\omega_{N,n} = \frac{\alpha\kappa}{8\pi}\{1 + C(1+\nu)N^{\nu}\}n. \tag{2}$$

Here, n is a positive integer, and κ is the surface gravity at the event horizon. As a result, such quantum black holes will have frequency-dependent reflectivity $R(\omega)$.

A. Gravitational perturbation

Although incorporating rotation in Eq. (2) is not a difficult job, we shall only focus on the nonrotating case. Then, our aim is to study perturbations on this black hole background as we modify the classical boundary condition at the horizon to model the absorption profile in terms of the characteristic frequencies given by Eq. (2). For this purpose, we consider a massless, quadrupole mode of the gravitational perturbation of the black hole. Then, the corresponding master equation for the perturbation $\Psi(x,t)$ is

$$[\partial_t^2 - \partial_x^2 + V_{\mathrm{Sch}}]\Psi(x,t) = 0, \tag{3}$$

where the effective potential is denoted by, $V_{\mathrm{Sch}}(r) = (6/r^2)(1-2M/r)(1-M/r)$. It is a well-known fact that this potential has its maximum at $r = 3M$, which signifies the location of the light ring. As we shall see, this light ring will play a crucial role in the formation of the black hole echo spectrum. Moreover, we have introduced the tortoise coordinate outside the horizon at $r = 2M$ as $x(r) = r + 2M\log(r/2M - 1)$.

Now, using a Fourier transformation of the perturbation, $\Psi(x,t) \coloneqq \int d\omega \tilde{\Psi}(x,\omega)e^{-i\omega t}$, we can cast the master equation into its most useful form:

$$-\partial_x^2\tilde{\Psi}(x,\omega) = [\omega^2 - V_{\mathrm{Sch}}(x)]\tilde{\Psi}(x,\omega). \tag{4}$$

It is interesting to notice the close resemblance of Eq. (4) with the time-independent Schrodinger equation. We want to study this equation with an outgoing boundary condition near spatial infinity—i.e., $\tilde{\Psi} \propto e^{i\omega x}$ as $x \to \infty$. However, we should be careful in fixing the boundary condition near the horizon, as the physics there will be modified due to the quantum effects sourced by the area quantization. It is reasonable to assume that these quantum modifications will only be important very close to the horizon—say, up to a radius $r < r_\epsilon = 2M(1+\epsilon)$ for some positive values of $\epsilon \ll 1$. For our purpose, we must set a reflecting boundary condition at $x = x_\epsilon \coloneqq x(r_\epsilon)$:

$$\tilde{\Psi}(x_\epsilon,\omega) \propto e^{-i\omega(x-x_\epsilon)} + R(\omega)e^{i\omega(x-x_\epsilon)}, \tag{5}$$

where $R(\omega)$ is the frequency-dependent reflectivity of the boundary at $r = r_\epsilon$. The classical result is obtained in the limit $R(\omega) = 0$.

B. Modeling the quantum filter

Quantization of the black hole area demands that the absorption occur only at the characteristic frequencies

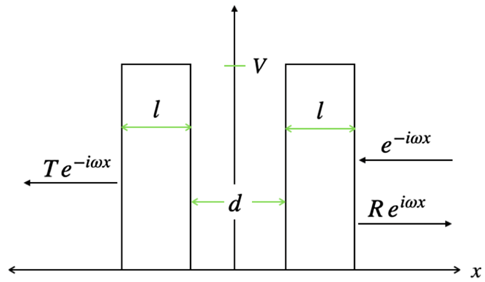

FIG. 1. Symmetric double-barrier potential with (rescaled) height V.

implying $R(\omega_{N,n}) = 0$, and otherwise $R(\omega) = 1$. Therefore, the absorption spectrum of a quantum black hole consists of sharply peaked lines about its characteristic frequencies $\omega = \omega_{N,n}$ given by Eq. (2). As suggested in Ref. [7], this behavior can be modeled by a quantum-mechanical double-barrier potential with a suitable choice of the barrier parameters—namely, its height V, width l, and separation d (see Fig. 1). However, in Ref. [7], the area quantization is assumed to be uniform, whereas we are considering the effect of the nonuniformity.

In order to mimic the black hole case, we must choose the double-barrier parameters so that the transmissivity $T(\omega)$ is very close to unity if $\omega = \omega_{N,n}$ given by Eq. (2). For any other frequency, $T(\omega)$ should be vanishingly small. For this purpose, it is instructive to calculate the transition amplitude $t(\omega)$ by comparing the situation with the similar problem in quantum mechanics. Using the result derived in Ref. [32], we may write (setting $c = 1$)

$$t = \frac{e^{-i\omega(d+2l)}}{e^{i\omega d}\mathcal{A} + e^{-i(\omega d-\delta)}\mathcal{B}}, \tag{6}$$

with $\mathcal{A} = \mathcal{M}^2 \sinh^2(\beta l)$ and $\mathcal{B} = \cosh^2(\beta l) + \mathcal{K}^2 \sinh^2(\beta l)$. We have also defined $\tan(\delta) = \mathcal{K}\sinh(2\beta l)[\cosh^2(\beta l) - \mathcal{K}^2\sinh^2(\beta l)]^{-1}$.

Here, we are using a rescaled version of the potential in order to make the aforesaid comparison possible: $(2m/\hbar^2)U = V$, where U is the actual potential that appears in the Schrodinger equation. Also, we have defined $\beta^2 = V - \omega^2$. Since the rescaled energy of the particle, $(2m/\hbar^2)E = \omega^2$, is less than the height of the potential barrier V, the quantity β is a positive real number. We have also used the notations $2\mathcal{M} = \beta/\omega + \omega/\beta$ and $2\mathcal{K} = \beta/\omega - \omega/\beta$.

Now, it is easy to calculate the transition probability, which is defined by the equation $T^2 = t\bar{t}$:

$$T^{-2} = \mathcal{A}^2 + \mathcal{B}^2 + 2\mathcal{A}\mathcal{B}\cos(2\omega d - \delta). \tag{7}$$

Thus, the transition probability is an oscillatory function having two envelopes defined according to the maxima and minima of the sinusoidal part. The equations of these envelopes are as follows:

$$\begin{aligned} \text{Upper envelope:}\ & |T|_u = (\mathcal{A} - \mathcal{B})^{-1} = 1, \\ \text{Lower envelope:}\ & |T|_l = [2\mathcal{M}^2\sinh^2(\beta l) + 1]^{-1}. \end{aligned} \tag{8}$$

Therefore, this double-barrier model mimics the event horizon of the quantum Schwarzschild black hole if we can choose the barrier separation (d) so that $T(\omega_{N,n}) = T_u = 1$. This demands a condition on the barrier separation d, as $2\omega_{N,n}d - \delta = (2s+1)\pi$. Using this condition, we get

$$\omega_{N,n} = \frac{s\pi}{d} + \frac{\delta + \pi}{2d}. \tag{9}$$

We should also check whether T_l given in Eq. (8) is vanishingly small, so that $T(\omega) = T_l \approx 0$ when $\omega \neq \omega_{N,n}$. For a fixed value of the particle's energy, this can be assured by choosing larger and larger heights of the potential barrier —i.e., $V \gg \omega^2$. In this limit, the phase of the sinusoidal part in the transition amplitude becomes $\delta_r = r\pi$ for some integers r. Then, Eq. (9) gives

$$\omega_{N,n} = \left(s + \frac{r}{2}\right)\frac{\pi}{d} + \omega_0, \tag{10}$$

where we define $\omega_0 = \pi/(2d)$. Next, we use Eq. (2) to obtain a direct relationship between the parameters of the double-barrier potential on the horizon and the quantization model of the area as

$$\frac{\alpha\kappa}{8\pi}\{1 + C(1+\nu)N^\nu\}n = \left(s + \frac{r}{2}\right)\frac{\pi}{d} + \omega_0. \tag{11}$$

To proceed further, we note that our main purpose is to study the late-time echo spectrum of the perturbation. For studying these echoes, we shall consider the initial wave-form to be a Gaussian that consists of all the modes $\omega_{N,n}$. Thus, our model makes better sense and simplifies if the barrier separation (d) does not carry any mode index. In other words, the n dependency must cancel out from both sides of the above equation. This task is achieved by first identifying the integers $n = r = s$, and then by making a constant shift in the frequency scale—i.e., by redefining $\omega \to \omega + \omega_0$.

Finally, Eq. (11) reads for nonuniform area quantization as

$$d = d_{\text{uniform}} \times [1 + C(1+\nu)N^\nu]^{-1}, \tag{12}$$

where $d_{\text{uniform}} = 12\pi^2/(\alpha\kappa)$ is the corresponding quantity for uniform area quantization. This equation gives a one-to-one correspondence between the width of the double-barrier potential and the model of quantization labeled by the quantization parameters (C, ν). Note that the exact value of the quantity α depends on the details of the quantization. In his original proposal [4], Bekenstein considered its value to be 8π, which is motivated by the transitions of a Schwarzschild black hole between different energy levels at discrete quasinormal mode frequencies [33,34]. However, other values of α are also studied in the literature [34].

Interestingly, Eq. (12) may provide us an important tool to distinguish the effects of nonuniform quantization from those of a uniform one in black hole echo. Uniform quantization gives a universal value for the quantity κd, for all Schwarzschild black holes. This universality is lost once the quantization is nonuniform and its value depends on the black hole mass through N. Therefore, for a given value of α, measuring the echo spectrum from multiple observations may provide us with knowledge about the values of d. We can then check how different its value is from d_{uniform}. In fact, future echo observations may also be useful in putting stark bounds on model parameters (C, ν).

One way to employ this idea is to plot the quantity κd for different values of N, which correspond to different black hole configurations. Then, the uniform quantization is represented by a horizontal line parallel to the N axis with an intercept of $(12\pi^2/\alpha)$ with the vertical axis. In contrast, any deviation from this horizontal line would indicate nonuniform quantization.

If we demand the correction to the area law to only be in the subleading order, Eq. (2) suggests that we should choose the values of (C, ν) so that $|C(1+\nu)N^{\nu}| < 1$. Moreover, as discussed in Ref. [18], for enriching the absorption spectrum, it is recommended to choose $C < 0$ rather than $C > 0$. All these considerations cause the quantity $[1 + C(1+\nu)N^{\nu}]$ to lie in the interval (0,1). Interestingly, from Eq. (12) we can infer that the more this quantity goes away from unity, the larger the separation between d and d_{uniform} becomes for the lower values of N (corresponding to black holes of a few solar masses). Thus, the subleading correction of the area law forces the echo measurement for nonuniform quantizations to stand out vividly from the uniform one. However, as N increases, the separation narrows gradually, to disappear at $N \to \infty$.

III. BLACK HOLE ECHOES

Formation of black hole echoes crucially hinges upon two important ingredients: the event horizon and the light ring. Among them, the latter remains unaffected by the process of area quantization, and it is located at $r = 3M$. The former is modeled by the double-barrier potential to mimic the selective absorption spectrum of the black hole. Owing to this quantum filter, any perturbation of frequencies other than what are given by Eq. (2) will be reflected back from the rightmost barrier wall of the potential, which signifies the extent of the quantum regime outside the black hole. It is important to note its dissimilarity from the reflection at a classical reflective surface that works as an amplitude divider. In other words, any radiation, irrespective of its frequency, is partly reflected and partly transmitted through a classical barrier. In contrast, the horizon of an area-quantized black hole works as a frequency filter. As a result, radiation of a particular frequency will be either absorbed or reflected completely, but not both simultaneously.

When the left-bound initial perturbation (taken in the form of a Gaussian waveform) reaches the light ring at $r = 3M$, it excites the photon sphere modes. This, in turn, results in the initial ringdown signals. After a certain time, these initial ringdown signals are reflected back from the barrier and come back to the light ring, where it partially transmits through the potential maximum of V_{Sch} [see Eq. (4)], and the remaining part is reflected back towards the horizon. As the process repeats itself, a series of black hole echoes is produced.

A. Placing the quantum filter

The duration between two consecutive echo signals—namely, the echo time—is roughly given by twice the light travel time between the double-barrier boundary and the light ring. However, depending on details of the near-horizon physics, this separation can depend on the model of area quantization. In fact, we have two distinct ways of placing the double-barrier quantum filter near the horizon. As we shall see, these two perspectives will give rise to significantly distinct echo spectra.

The first model is closely related to what is depicted in Ref. [7], where the rightmost barrier wall of the potential is aligned with the surface of quantum extent located at $x = x_\epsilon$. In this model, we assume that the location of x_ϵ that acts as a reflecting surface is model-independent and can be fixed universally for all Schwarzschild black holes of mass M. However, due to the model dependency of the barrier separation d given by Eq. (12), the location of the inner barrier wall may vary; see Fig. 2. We can think of the inner barrier wall as the location of the modified absorption surface $x_A(C, \nu)$ due to the quantum effects near the

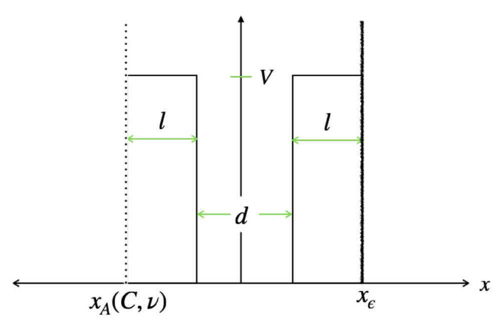

FIG. 2. Model 1: The dotted line represents the absorption surface that varies with (C, ν), and the thick line denotes the fixed reflection surface.

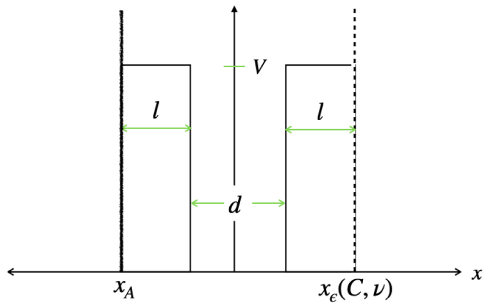

FIG. 3. Model 2: The dotted line represents the reflection surface that varies with (C, ν), and the thick line denotes the fixed absorption surface.

horizon. Since the distance between the reflecting surface x_ϵ and the location of the light ring does not vary with different choices of (C, ν), the echo time is independent of the nature of area quantization. In other words, nonuniform area quantization leads to the same echo time as that of uniform quantization.

The universality of the echo time can be lifted by introducing an alternative perspective. In this model, we consider the location of the absorption surface at x_A to be fixed and model independent. However, the location of the reflecting surface x_ϵ is now varying due to the change of the barrier separation d as given by Eq. (12); for different choices of model parameters (C, ν), see Fig. 3. As a result, the separation between x_ϵ and the light ring becomes model dependent, and so is the echo time.

However, in any case, we need to be careful so that the values of x_A and x_ϵ are indeed close to the horizon and inside the quantum regime.

B. Cauchy evolution equation

In both the models, to find the echoes, we need to express the time-domain master equation for the perturbation in double-null coordinates defined by $u \coloneqq t - x$ and $v \coloneqq t + x$ in the units of $c = 1$. In these coordinates, Eq. (3) takes the form

$$[4\partial_u \partial_v + V]\Psi(u, v) = 0. \tag{13}$$

Here, the potential V consists of two parts: the classical Schwarzschild potential V_{Sch}, and the quantum filter V_{Barrier} near the horizon. The second part is required to incorporate the quantum boundary condition at the boundary at $x = x_\epsilon$. Thus, the perturbation evolves under the influence of the combined potential $V = V_{\mathrm{Sch}} + V_{\mathrm{Barrier}}$. To solve Eq. (13) numerically, we discretize the (u, v) plane in the form of a square grid of length $h \ll 1$. Then, the evolution equation becomes

$$\begin{aligned}\Psi(u+h, v+h) = {} & \Psi(u+h, v) + \Psi(u, v+h) - \Psi(u, v) \\ & - \frac{h^2}{8}[V(u+h, v)\Psi(u+h, v) \\ & + V(u, v+h)\Psi(u, v+h)].\end{aligned} \tag{14}$$

Using this equation, we can now study the evolution of an initial Gaussian waveform in order to find the black hole echo spectrum.

C. The echo spectrum

We begin with an analysis of the echo time Δt_{echo} for both the models. As discussed before, the echo time is roughly twice the light travel time between the light ring and the rightmost barrier of the quantum filter. In the leading order, it is given by

$$M^{-1}\Delta t_{\mathrm{echo}} \sim 2[1 - 2\ln 2 - 2\epsilon + 2\ln(\epsilon^{-1})]. \tag{15}$$

Note that the quantity $M^{-1}\Delta t_{\mathrm{echo}}$ has no explicit dependence on mass M; the only dependence on mass may come implicitly through the parameter ϵ in the context of model 2.

In model 2, the absorption surface is fixed at a distance $r_A = 2M(1 + a)$, where $a < \epsilon \ll 1$. Then, the extent of the quantum region is governed by the following equation:

$$\epsilon(C, \nu) = a\mathrm{Exp}\left[\frac{24\pi^2}{\alpha(1 + CN^\nu(1 + \nu))}\right]. \tag{16}$$

Thus, for a given mass M, the quantum extent outside the horizon (ϵ) can vary with different choices of quantization parameters (C, ν). Also, for a fixed choice of the parameters $(C \neq 0, \nu)$, the extent ϵ will be different for different masses via N.

In contrast, for model 1, ϵ is a constant parameter independent of (M, C, ν) and is fixed only by the quantum extent outside the event horizon. We also point out that in both the models, Eq. (15) gives the same value of $M^{-1}\Delta t_{\mathrm{echo}}$ for uniform quantization $(C = 0)$.

Now, let us consider the echo spectrum for the two models separately. Figure 4 shows the echo spectrum corresponding to model 1, for both uniform and nonuniform area quantizations. As is expected, the echo wavefronts are almost identical, revealing no information about the model parameters C and ν. This is because the distance between the reflecting surface x_ϵ and the location of the light ring does not vary with (C, ν). As a consequence, the echo time Δt_{echo} is unaltered for different models and depends only on the mass M of the black hole. In fact, in the leading order, the quantity $M^{-1}\Delta t_{\mathrm{echo}}$ does not depend on the mass.

The situation for model 2 is depicted in Fig. 5. This is the case when the location of the absorption surface at x_A is fixed and model independent, and the reflecting surface x_ϵ is varying due to different choices of model parameters

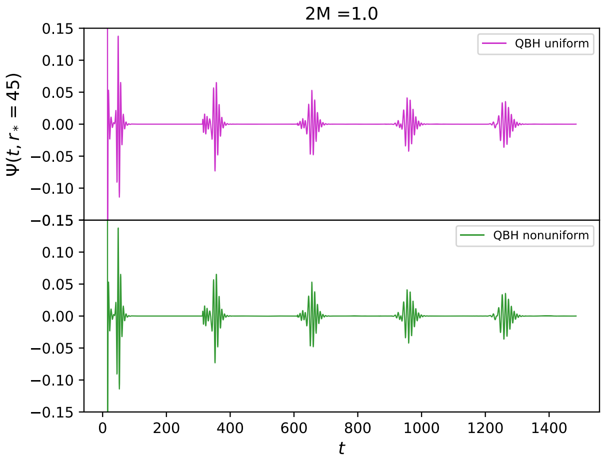

FIG. 4. Gravitational wave echo spectrum for model 1. The parameters for the nonuniform quantization are $C = -3.6$ and $\nu = -1/90$. We have chosen $\epsilon = 10^{-59}$.

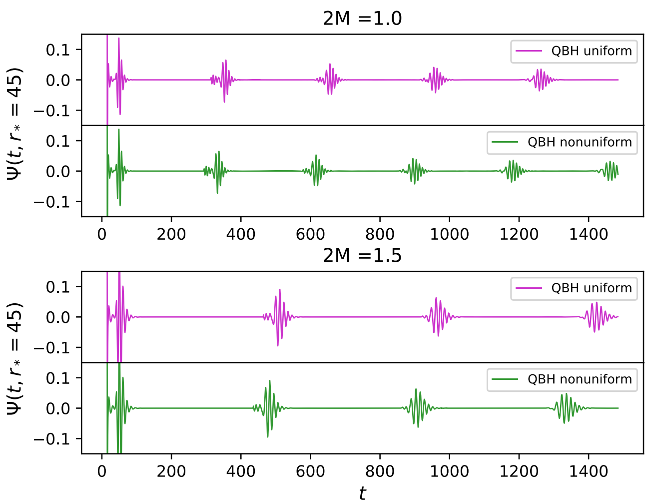

FIG. 5. Gravitational wave echo spectrum for model 2. The parameters for the nonuniform quantization are $C = -3.6$ and $\nu = -1/90$. We have chosen $a = 10^{-70}$.

(C, ν). As a result, the echo time, the time separation between two consecutive echoes, depends on the nature of quantization. In fact, this immediately suggests a possible test to distinguish these two models.

In the context of model 2, if the gravitational echo is observed by future detectors for more than one GW source, a significant variation of the quantity $M^{-1}\Delta t_{\mathrm{echo}}$ will be a strong evidence for nonuniform area quantization. This is quite explicit in an order-of-magnitude estimation of the echo time for model 2, $M^{-1}\Delta t_{\mathrm{echo}} \sim 4\ln(\epsilon_{\max}/\epsilon)$. Here, the quantity $\epsilon_{\max} = \sqrt{e}/2$ can be fixed universally. Interestingly, the positivity of echo time gives an upper bound on ϵ for a given choice of (C, ν): $\epsilon < \epsilon_{\max}$. This bound can be translated to a upper bound on the parameter a that signifies the location of the absorption surface:

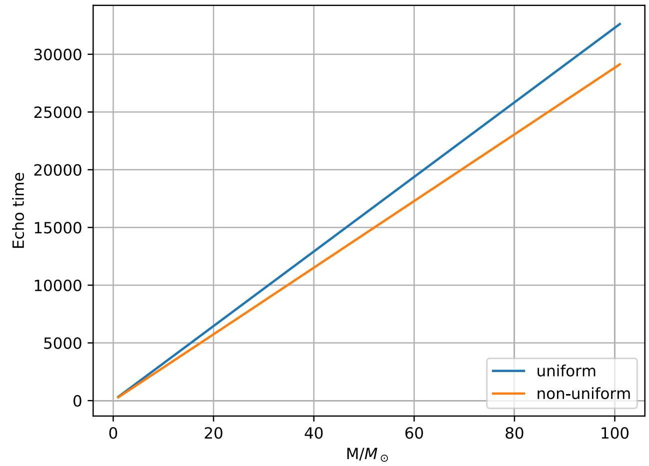

FIG. 6. Variation of echo time (in units of solar mass $M_{\odot}$) with mass of the black hole for model 2. The parameters for the nonuniform quantization are $C = -3.6$ and $\nu = -1/90$.

$$a_{\max} = \frac{\sqrt{e}}{2}\mathrm{Exp}\left[-\frac{24\pi^2}{\alpha(1 + CN^{\nu}(1+\nu))}\right]. \tag{17}$$

There is no such bound on ϵ for model 1, since the echo time is always positive.

Figure 6 shows the variation of the echo time with black hole mass for model 2. There is a noticeable difference between uniform and nonuniform area quantizations for higher values of the black hole mass.

In order to distinguish between these two models depending on the placement of the quantum filter near the horizon, and also between the uniform and nonuniform area quantizations, we may proceed as follows: First, from the gravitational echo observations by future detectors, we may investigate the variation of the quantity $M^{-1}\Delta t_{\mathrm{echo}}$ for multiple GW sources of different masses. If it varies significantly for different sources, then model 2 is preferred over model 1. Subsequently, we try to fit the observed echo time data with theoretically expected values in model 2 for different choices of (C, ν). If the best-fit model parameter significantly differs from $C = 0$, it would suggest that the black hole area quantization is nonuniform.

IV. CONCLUSION

In this paper, we have explored the effects of both uniform and nonuniform area quantization on GW echoes from a perturbed black hole. As a result of area discretization, black holes deviate from their classical behavior and absorb selectively at certain characteristic frequencies. Motivated by the method presented in Ref. [7], we model this selective absorption using a double-barrier potential placed near the horizon. We show that, depending on the near-horizon physics, there are two distinct ways to place the potential barrier, which lead to drastically different consequences on the echo spectrum. The echo profile—and in particular, the echo time—is sensitive to the quantization parameters (C, ν) for only one of these models—namely, model 2. In that case, the echo time Δt_{echo} scales nonlinearly with the mass and potentially offers an observational test to distinguish between these two models. In fact, since Δt_{echo} does not depend on the parameters (C, ν) for model 1, a parameter estimation for (C, ν) should return only $C = 0$. On the other hand, model 2 may allow nonzero values of C.

Note that we have only considered power-law corrections to the area-entropy proportionality, motivated by Refs. [14–16]. Interestingly, a logarithmic correction to the entropy will not have any detectable effects. This is similar to the inspiral case, as pointed out in Ref. [18].

It will be interesting if we can generalize our analysis beyond spherical symmetry and for more general black hole spacetimes. An extension for black holes of higher-curvature gravity theories may also be useful.

ACKNOWLEDGMENTS

K. C. acknowledges the use of the cluster Noether at IIT Gandhinagar. The research of R. G. is supported by the Prime Minister Research Fellowship (No. PMRF-192002-120), Government of India. The research of S. S. is supported by the Department of Science and Technology, Government of India under a SERB CRG Grant (No. CRG/2020/004562).

[1] B. P. Abbott *et al.* (LIGO Scientific and Virgo Collaborations), Phys. Rev. Lett. **116**, 061102 (2016).
[2] B. P. Abbott *et al.* (LIGO Scientific and Virgo Collaborations), Phys. Rev. Lett. **116**, 221101 (2016); **121**, 129902(E) (2018).
[3] I. Agullo, V. Cardoso, A. D. Rio, M. Maggiore, and J. Pullin, Phys. Rev. Lett. **126**, 041302 (2021).
[4] J. D. Bekenstein, Lett. Nuovo Cimento **11**, 467 (1974).
[5] J. D. Bekenstein and V. F. Mukhanov, Phys. Lett. B **360**, 7 (1995).
[6] V. F. Foit and M. Kleban, Classical Quantum Gravity **36**, 035006 (2019).
[7] V. Cardoso, V. F. Foit, and M. Kleban, J. Cosmol. Astropart. Phys. 08 (2019) 006.
[8] S. Datta, K. S. Phukon, and S. Bose, Phys. Rev. D **104**, 084006 (2021).
[9] S. Datta and K. S. Phukon, Phys. Rev. D **104**, 124062 (2021).
[10] S. W. Hawking, Phys. Rev. Lett. **26**, 1344 (1971).
[11] R. M. Wald, Phys. Rev. D **48**, R3427 (1993).
[12] S. Sarkar, Gen. Relativ. Gravit. **51**, 63 (2019).
[13] L. Bombelli, R. K. Koul, J. Lee, and R. D. Sorkin, Phys. Rev. D **34**, 373 (1986).
[14] S. Das and S. Shankaranarayanan, Phys. Rev. D **73**, 121701 (2006).
[15] S. Das, S. Shankaranarayanan, and S. Sur, Phys. Rev. D **77**, 064013 (2008).
[16] S. Sarkar, S. Shankaranarayanan, and L. Sriramkumar, Phys. Rev. D **78**, 024003 (2008).
[17] D. Kothawala, T. Padmanabhan, and S. Sarkar, Phys. Rev. D **78**, 104018 (2008).
[18] K. Chakravarti, R. Ghosh, and S. Sarkar, Phys. Rev. D **104**, 084049 (2021).
[19] V. Cardoso, E. Franzin, and P. Pani, Phys. Rev. Lett. **116**, 171101 (2016).
[20] V. Cardoso, S. Hopper, C. F. B. Macedo, C. Palenzuela, and P. Pani, Phys. Rev. D **94**, 084031 (2016).
[21] V. Cardoso and P. Pani, Nat. Astron. **1**, 586 (2017).
[22] Z. Mark, A. Zimmerman, S. M. Du, and Y. Chen, Phys. Rev. D **96**, 084002 (2017).
[23] M. R. Correia and V. Cardoso, Phys. Rev. D **97**, 084030 (2018).
[24] P. Bueno, P. A. Cano, F. Goelen, T. Hertog, and B. Vercnocke, Phys. Rev. D **97**, 024040 (2018).
[25] J. Abedi, H. Dykaar, and N. Afshordi, Phys. Rev. D **96**, 082004 (2017).
[26] J. Abedi, H. Dykaar, and N. Afshordi, arXiv:1701.03485.
[27] R. S. Conklin, B. Holdom, and J. Ren, Phys. Rev. D **98**, 044021 (2018).
[28] J. Westerweck, A. Nielsen, O. Fischer-Birnholtz, M. Cabero, C. Capano, T. Dent *et al.*, Phys. Rev. D **97**, 124037 (2018).
[29] K. W. Tsang, M. Rollier, A. Ghosh, A. Samajdar, M. Agathos, K. Chatziioannou *et al.*, Phys. Rev. D **98**, 024023 (2018).
[30] A. B. Nielsen, C. D. Capano, O. Birnholtz, and J. Westerweck, Phys. Rev. D **99**, 104012 (2019).
[31] R. K. L. Lo, T. G. F. Li, and A. J. Weinstein, Phys. Rev. D **99**, 084052 (2019).
[32] E. H. Hauge, J. P. Falck, and T. A. Fjeldly, Phys. Rev. B **36**, 4203 (1987).
[33] S. Hod, Phys. Rev. Lett. **81**, 4293 (1998).
[34] M. Maggiore, Phys. Rev. Lett. **100**, 141301 (2008).